Available online at www.sciencedirect.com
ScienceDirect
Journal of Catalysis 251 (2007) 163–171
JOURNAL OF CATALYSIS
www.elsevier.com/locate/jcat

A bifunctional catalyst for the single-stage water–gas shift reaction in fuel cell applications. Part 2. Roles of the support and promoter on catalyst activity and stability

K.G. Azzam, I.V. Babich, K. Seshan, L. Lefferts *

Catalytic Processes and Materials, Faculty of Science and Technology, IMPACT, University of Twente, P.O. Box 217, 7500AE, Enschede, The Netherlands

Received 29 March 2007; revised 5 July 2007; accepted 8 July 2007

Available online 21 August 2007

Abstract

The nature of oxide supports has a crucial effect on the performance of Pt-based catalysts in the water–gas shift reaction. Supports not only determine the activity of the catalyst, but also influence their stability (deactivation mechanism). Among the catalysts studied, Pt/TiO_2 was the most active. Pt/CeO_2 deactivated with time due to the formation of stable carbonate on the ceria surface. Sintering of Pt was found to be the cause of Pt/TiO_2 deactivation. Using mixed oxides as catalyst supports did not improve the activity despite the better red–ox properties of mixed oxides compared with the single-oxide supports. Pt/TiO_2 could be stabilized by adding a second metal (Re), which prevented Pt sintering. In addition, $Pt–Re/TiO_2$ was more active than Pt/TiO_2. Under WGS conditions, part of the Re was present in oxidizing form (ReO_x); we speculate that this helped improve the catalyst activity.

Keywords: WGS reaction; Platinum; Rhenium; Tin; Oxide supports; Activity; Stability; Deactivation

1. Introduction

The water–gas shift (WGS) reaction, $CO + H_2O \Leftrightarrow CO_2 + H_2$, is applied in the conversion of syngas produced by steam reforming or partial oxidation of hydrocarbons to increase H_2 yield [1]. In recent years, there has been renewed interest in this reaction because of its potential for use in H_2-based fuel cells in mobile applications.

In Part 1 of this paper [2], we reported, based on spectroscopic and kinetic transient studies, that the support plays a crucial role in determining the WGS reaction sequence over Pt-based catalysts. These catalysts are thus bifunctional, with CO activated over metal platinum and H_2O activated over the support oxide surface [3–5]. Platinum has been reported to also facilitate the decomposition of intermediate surface formate in the presence of H_2O [6]. We showed earlier [2] that the nature of the support not only determined the mode of activation of H_2O (either by formation of surface hydroxyls or via oxidation of reduced support with H_2O forming H_2), but also affected the formation and stability of the intermediates (e.g., formates, carbonates) on the catalyst surface.

Various oxide supports that differ in terms of their reducibility or oxygen mobility (e.g., CeO_2 [6–10], TiO_2 [11], ZrO_2 [12]) supporting noble metals have been reported as promising WGS catalysts. Catalyst activity reportedly depends on catalyst preparation [6,11,13,14], catalyst testing conditions, and reactor designs [15].

Ceria has been reported as an oxide support with high red–ox capacity and mobility of surface oxygen/hydroxyl groups [16]. Reduction of Ce^{4+} to Ce^{3+} aids in the formation of bridging hydroxyls, which are claimed to be active for WGS reaction [6–10]. Our results of in situ IR and kinetic studies [2] confirmed that over Pt/CeO_2, the WGS reaction proceeds via the classical associative formate mechanism, in agreement with others [5–7].

Although titania is more resistant to reduction than ceria, it can be partially reduced under the WGS reaction conditions studied. Calatayud et al. [17] reported that reduction of TiO_2 is facile, resulting in creation of oxygen vacancies (defects) via reduction of the cation charge (Ti^{x+}, $x < 4$). We showed [2]

* Corresponding author.
E-mail address: l.lefferts@tnw.utwente.nl (L. Lefferts).

0021-9517/$ – see front matter
doi:10.1016/j.jcat.2007.07.011

that the oxygen vacancies over Pt/TiO_2 catalyst, formed by the reduction with CO, could dissociate H_2O to H_2 and regenerate surface oxygen sites and also form hydroxyl groups. For Pt/TiO_2, both the classical red–ox route and the associative formate route with red–ox regeneration [2] are possible reaction pathways for the WGS reaction.

Although ZrO_2 is a difficult-to-reduce oxide [18], it can form hydroxyl groups in the presence of water [19]. Nevertheless, we demonstrated that surface oxygen on ZrO_2 catalyst is reactive at the WGS reaction temperature (300 °C) [2].The dominant reaction pathway is the associative formate route with red–ox regeneration.

Thus, WGS reaction in the case of Pt/TiO_2 and Pt/ZrO_2 catalysts follows a pathway which includes a red–ox step. Red–ox properties of bulk oxides can be effectively modified by incorporating dopant atoms. It has been shown [20,21] that incorporation of Zr into CeO_2 lattice promotes the red–ox properties of the support. Recently, Ruettinger et al. [22] reported that adding Zr to CeO_2 improved the catalyst performance in the WGS reaction by suppressing carbonate buildup on the CeO_2 surface. Dong et al. [23] found that palladium supported over ceria–titania mixed oxides (Pd/CeO_2–TiO_2) have superior activity for CO oxidation compared with Pd/CeO_2 or Pd/TiO_2 under the same conditions. These findings suggest that manipulating the red–ox properties of the supports and surface oxygen mobility could be a way to improve catalyst performance.

Investigation of mechanistic pathways over supported Pt catalysts in Part 1 [2] indicate that water activation can follow different sequences (hydroxyl formation vs red–ox water splitting) and thus influence catalytic activity. Further, we showed that the support influences the reaction pathway (formate vs red–ox routes), which also may result in different catalytic activities. In addition, the formation of carbonate-type species on the support block sites for water activation and are detrimental to catalyst stability. Thus, studies on WGS catalysts based on supports with varying red–ox properties, hydroxyl formation, and carbonate stability would be useful in designing efficient WGS catalysts.

In this work, we report on the activity, selectivity, and stability of the Pt-based catalysts studied in Part 1, along with catalysts with enhanced red–ox properties based on mixed oxides. We investigate deactivation scenarios for different supports and describe possible ways to regenerate and stabilize catalyst activity.

2. Experimental

2.1. Catalyst preparation

This study used commercial supports: TiO_2 (Degussa, P-25), CeO_2 (Aldrich), and ZrO_2 (Daiichi Kagaku Kogyo, RC100). A series of mixed-oxide supports were prepared in our laboratory. $Ce_xZr_{1-x}O_2$ ($x = 0.2$, 0.5) solid solutions were prepared by co-precipitation using appropriate ratios of $Ce(NO_3)_3{\cdot}6H_2O$ (99.99% Aldrich) and $ZrOCl_2$ (99.9% ABCR) [20]. Mixed $Ti_xCe_{1-x}O_2$ and $Ti_xZr_{1-x}O_2$ ($x = 0.2$, 0.5) were prepared by the sol–gel method using an ethanol solution of titanium (IV) iso-propoxide (98%) and an aqueous solution of $Ce(NO_3)_3{\cdot}6H_2O$ (0.4 M) or $ZrOCl_2$ (0.4 M). The precursor solutions were mixed in appropriate amounts at room temperature and left for 24 h to form a gel. After gelation, the samples were dried under vacuum in a rotary evaporator at 75 °C for 3 h. All of the supports were calcined at 500 °C for 4 h before Pt was incorporated.

The monometallic catalysts were prepared by wet impregnation of supports with aqueous solutions of H_2PtCl_6. Required amounts of H_2PtCl_6 solution were used to yield catalysts with 0.5 wt% Pt. The bimetallic (Pt/Re and Pt/Sn) TiO_2 catalysts were prepared with 0.5 wt% of Pt and a Pt/Re or Pt/Sn molar ratio close to unity. TiO_2 was first impregnated first with the required concentration of NH_4ReO_4 or $SnCl_2{\cdot}2H_2O$ for 1 h at room temperature and then contacted with H_2PtCl_6 before drying to yield 0.5 wt% Pt–0.48 wt% Re/TiO_2 and 0.5 wt% Pt–0.3 wt% Sn/TiO_2 catalysts, respectively. All catalysts prepared in this study were dried at 75 °C for 2 h under vacuum in a rotary evaporator and subsequently calcined at 450 °C for 4 h (at a heating rate of 10 °C min^{-1}).

2.2. Characterization

The surface areas of the catalysts were measured by the BET method using a Micromeritics ASAP 2400 device. Platinum loading was determined using a Philips PW 1480 X-ray fluorescence spectrometer. Pt dispersion for all of the catalysts except Pt–Re/TiO_2 was determined by H_2 chemisorption at room temperature using a Micromeritics Chemisorb 2750. Teschner et al. [24] showed in a detailed study that significant hydrogen spillover did not occur on Pt/CeO_2 at lower temperatures (e.g., 20 °C), resulting in reliable dispersion measurements. This demonstrates that H_2 spillover from Pt particles to the support surface does not influence dispersion measurements in the ceria-supported catalysts. CO chemisorption at room temperature was used to measure the dispersion of Pt in Pt–Re/TiO_2 catalyst based on the findings of Pieck et al. [25] and Carvalho et al. [26]. Based on a comparison of Pt particle size measured by H_2 or CO chemisorption with TEM results, these authors reported that adding Re to Pt decreased the chemisorption capacity of H_2. They found that Pt particle size was comparable with CO chemisorption and TEM but was much larger with H_2 chemisorption; this result did not match the TEM data. Moreover, Re did not chemisorb CO at 30–50 °C [25]. This is also in agreement with our IR results (not shown) on Pt–Re/TiO_2, showing that CO was adsorbed on Pt only at room temperature.

The platinum particle size for Pt/TiO_2 and Pt–Re/TiO_2 catalysts was also measured by TEM using a Philips CM30 microscope, with the sizes of about 30 particles averaged. The oxidation state of rhenium in Pt–Re/TiO_2 catalyst was characterized by XPS using a Φ Quantera Scanning ESCA Microprobe spectrometer using AlK_α (1486.7 eV, 25.64 W).

Temperature-programmed reduction (H_2-TPR) studies were conducted in a Micromeritics Autochem II 2920 device. Here, 1 g of catalyst was placed in a U-quartz tube and preheated to 300 °C, then cooled to −75 °C under Ar flow (20 ml/min). Once the TCD signal was stabilized, the feed was switched to

15% H_2/Ar flow (20 ml/min). The temperature of the sample was raised from −75 to 850 °C at a constant rate of 10 °C/min.

2.3. Catalytic tests

Catalytic tests for WGS reaction were carried out in a fixed-bed quartz tubular reactor (3 mm i.d.) under differential conditions. Typically, the catalysts were pressed into pellets, crushed, and sieved to yield grains of 0.25–0.3 mm diameter. A 10-mg catalyst sample diluted with 90-mg quartz grains (0.25–0.30 mm) was packed between two layers of quartz wool. Using the quartz grains ensured plug flow criterion and minimized the effect of heat generated by the exothermic reaction. The temperature of the catalyst bed was monitored by thermocouples (Fe–Cr) and maintained by a temperature controller (Eurotherm 2416). All catalysts were first reduced in 10% H_2 in N_2 (total flow, 100 ml/min) for 30 min and subsequently purged with N_2 for another 30 min at 300 °C. All gases used (He, H_2, N_2, CO_2, and CO) were of >99.9% purity. A gas mixture containing 3 vol% CO, 7.5% H_2O, and N_2 balance was used for catalytic tests. Steam was provided to the system via a steam generator consisting of a hollow cylinder (50 mm i.d., 150 mm long) packed with quartz wool. Water was fed by a pulse-free syringe pump (ISCO series D) into the steam generator via a long (5 m) capillary tube to obtain a stable water concentration. The whole system was heated to 125 °C to avoid condensation of H_2O. The feed was adjusted in bypass mode to obtain constant $CO/H_2O/N_2$ (= 3/7.5/89.5 mol/mol%, N_2 as an internal standard) before the experiment. The total flow rate of the feed gas into the reactor was kept at 350 ml/min using Brooks mass flow controllers. The inlet and outlet gases (CO, CO_2, H_2, H_2O, and N_2) were analyzed using Varian Micro GC (CP4900) using MS5 and PPQ columns.

2.4. Pulse experiments

Kinetic transient pulse experiments were performed at 300 °C, using a fixed-bed reactor. The details were described in Part 1 [2].

3. Results and discussion

Physical and chemical characteristics of the catalysts such as BET surface area, composition (XRF), and Pt dispersion are summarized in Table 1. The surface area of the catalysts varied from 22 m^2/g for Pt/ZrO_2 to 147 m^2/g for $Pt/Ti_{0.8}Ce_{0.2}O_2$. All catalysts had comparable Pt dispersions of around 60 ± 5%, except for $Pt/Ti_{0.5}Zr_{0.5}O_2$ (45%), demonstrating that this set of catalysts with comparable Pt loadings and dispersions was suitable for determining the effect of the support on the catalytic performance.

3.1. Catalytic performance

To account for the small differences in Pt dispersions and loadings, catalyst activities are expressed in TOF (s^{-1}), the number of molecules converted (CO) or produced (H_2, CO_2) per surface Pt atom and per second. CO conversion was kept below 15%, working close to differential conditions. All catalysts tested were selective to H_2. Methane formation was below the limit of detection (<10 ppm), and the rate of hydrogen formation was equal to the rate of CO_2 formation (±2%).

Table 1
BET surface area, metal loading and Pt dispersion of the mono metallic catalysts used in this work

Catalyst (0.5 wt% Pt)	S_{BET} (m^2/g) support	XRF Pt (wt%)	H/Pt (%)
ZrO_2	22	0.47	60
$Ti_{0.5}Zr_{0.5}O_2$	145	0.53	45
$Ce_{0.8}Zr_{0.2}O_2$	100	0.52	63
$Ti_{0.8}Ce_{0.2}O_2$	147	0.49	65
CeO_2	81	0.54	65
$Ce_{0.5}Zr_{0.5}O_2$	107	0.58	62
$Ti_{0.5}Ce_{0.5}O_2$	88	0.50	60
TiO_2	48	0.49	55

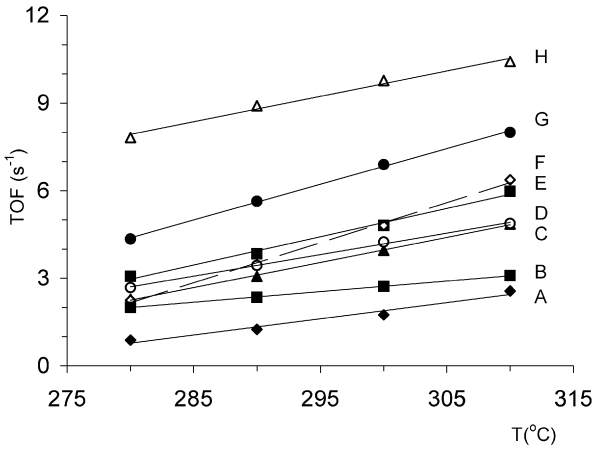

Fig. 1. Turn over frequency (TOF) for the WGS reaction on various catalysts using partial pressure of 60 and 150 mbar for CO and H_2O, respectively, $P = 2$ bar, and HSGV = 2,100,000 h^{-1}. Data are shown for 0.5 wt% of Pt on different supports: (A, ◆) ZrO_2; (B, ■) $Ti_{0.5}Zr_{0.5}O_2$; (C, ▲) $Ce_{0.8}Zr_{0.2}O_2$; (D, ○) $Ti_{0.8}Ce_{0.2}O_2$; (E, ■) CeO_2; (F, ◇) $Ce_{0.5}Zr_{0.5}O_2$; (G, ●) $Ti_{0.5}Ce_{0.5}O_2$; (H, △) TiO_2.

Fig. 1 presents the intrinsic activities by TOF for hydrogen formation during the WGS reaction over the catalysts studied. The figure shows, in agreement with other studies [5,27,28], that the oxide support had a strong influence on the rate of hydrogen formation. Among the catalysts studied, Pt/TiO_2 was the most active. Activity followed the order Pt on TiO_2 > $Ti_{0.5}Ce_{0.5}O_2$ > $Ce_{0.5}Zr_{0.5}O_2$ ~ CeO_2 > $Ti_{0.8}Ce_{0.2}O_2$ > $Ce_{0.8}Zr_{0.2}O_2$ > $Ti_{0.5}Zr_{0.5}O_2$ > ZrO_2. Recalling that the order of activity for single-oxide supports was Pt/TiO_2 > Pt/CeO_2 > Pt/ZrO_2, it can be seen that mixed-oxide supports did not result in enhanced catalytic performance. In order of activity, they are between that of single oxides, indicating performance of oxide mixtures. However, the red–ox capacity of $Pt/Ti_{0.5}Ce_{0.5}O_2$ was much higher than that of the individual Pt/TiO_2 or Pt/CeO_2, based on experiments with subsequent pulsing of CO and H_2O over $Pt/Ti_{0.5}Ce_{0.5}O_2$ catalyst (Fig. 2). This was substantiated by the amount of CO_2 formed during CO pulses (553, 68, and 51 μmol g^{-1} CO_2 for $Pt/Ti_{0.5}Ce_{0.5}O_2$, Pt/CeO_2, and Pt/TiO_2,

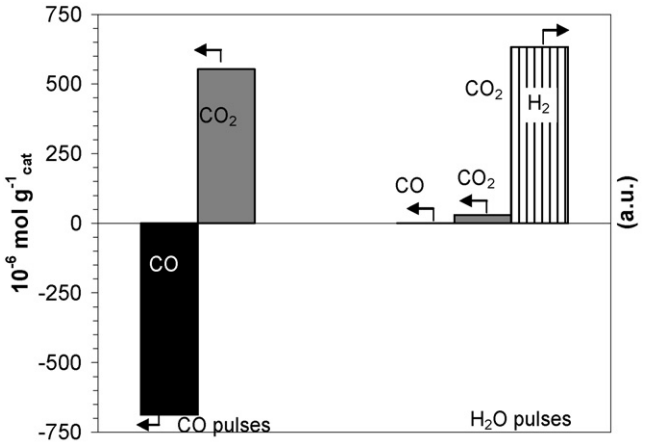

Fig. 2. CO and H_2O pulse results over 0.5% $Pt/Ti_{0.5}Ce_{0.5}O_2$ catalyst at 300 °C.

respectively [2]). Therefore, $Pt/Ti_{0.5}Ce_{0.5}O_2$ is not a physical mixture of Pt/TiO_2 and Pt/CeO_2. The mixed-oxide support must be, at least partially, a solid solution, influencing the catalytic properties as well as red–ox properties; unfortunately, XRD did not reveal any details. Based on these data, we can conclude that increasing the oxygen mobility and redox capacity of the support did not significantly improve catalyst performance under the WGS conditions that we studied.

Two Pt/TiO_2 catalysts with different Pt metal dispersions (55 and 35%) showed the same TOF for hydrogen formation (10 s^{-1} at 300 °C), indicating an absence of particle size effects on catalytic activity. We showed earlier [2] that the oxide support influences the mechanistic reaction sequence for the WGS reaction; thus, it is not surprising to see that the support oxide influenced the catalyst activity.

3.2. Catalyst deactivation

Catalyst stability with time on stream is one key factor that must be taken into account when considering commercial applications of the catalyst. For example, Pt/CeO_2 is often cited as the most promising single-stage WGS catalyst [7–9]. However, earlier studies have made little mention of catalyst stability. Fig. 3a shows changes in relative activity (normalized to its initial activity) for Pt/CeO_2, Pt/TiO_2, Pt/ZrO_2, and $Pt/Ti_{0.5}Ce_{0.5}O_2$, comparing initial catalyst activity, activity after 20 h on a WGS reaction stream, and activity after regeneration of the used catalyst with O_2 at 450 °C. Fig. 3b shows Pt dispersions for these catalysts before and after the 20-h activity tests. All of the catalysts except Pt/ZrO_2 lost about 40% of their initial activity after 20 h of testing. Pt/ZrO_2 showed stable activity; recall, however, that it had the lowest activity (see Fig. 1). Therefore, it was not considered for further study.

Because the oxide-supported Pt catalysts are bifunctional in the WGS shift reaction [2,4,5,27,28], loss of activity may be caused by deactivation of Pt or oxide surface sites, or both. In Pt/CeO_2, no Pt sintering was observed during time on stream. The Pt dispersion was 65% on fresh catalyst and 67% on used catalyst (see Fig. 3b), even though the catalyst showed strong deactivation. Oxidative treatment at 450 °C for 1 h al-

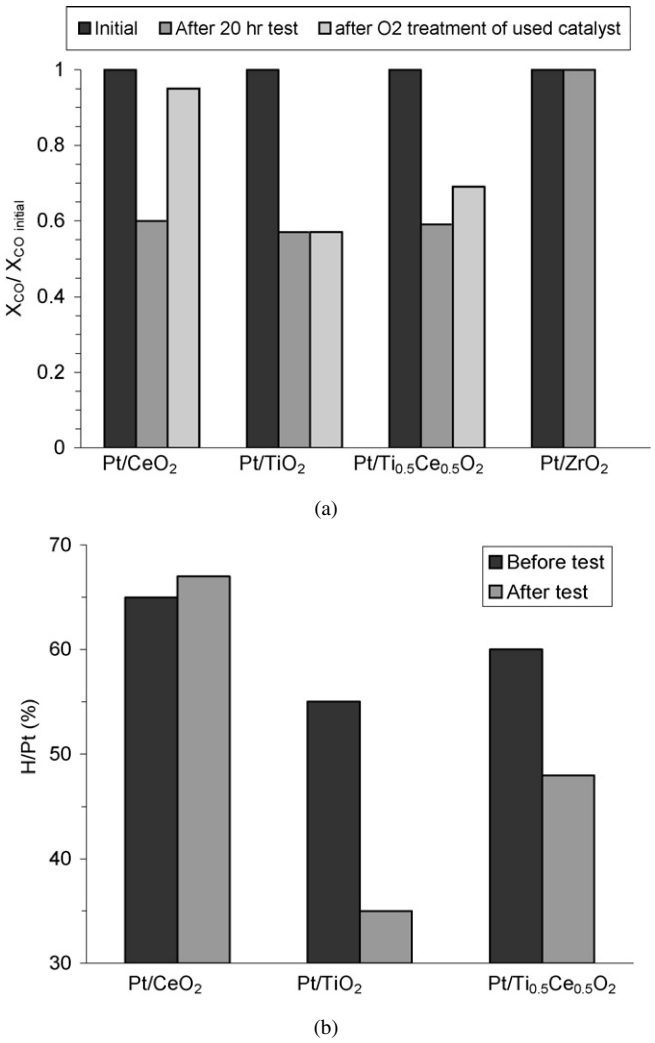

Fig. 3. (a) WGS CO conversion (normalized) at 300 °C as for Pt/CeO_2, Pt/TiO_2 and $Pt/Ti_{0.5}Ce_{0.5}O_2$; conditions: partial pressure of 60 and 150 mbar for CO and H_2O, respectively, $P = 2$ bar, and GHSV = 1,025,000 h^{-1}. (b) Pt dispersion; before test and after 20 h test on the stream.

lowed almost complete recovery (95%) of initial catalyst activity (Fig. 3a). As shown earlier [2], stable oxygenates (formate and/or carbonate) are formed on ceria while contacting the catalyst with CO. Moreover, on Pt/CeO_2, part of the "C"-containing species was retained on the surface even in the presence of H_2O at 300 °C. Because formate is reactive in the presence of H_2O, we concluded [2] that the "C" specie must consist mainly of carbonates:

$$CO_2 + O_{(s)} \rightleftarrows CO_{3(s)}. \quad (1)$$

This is in agreement with the stability of cerium carbonate up to 430 °C under WGS conditions [29].

Our conclusion is also in agreement with the findings of Liu et al. [29], who reported instability of the Pt/CeO_2 catalyst during startup and shutdown cycles due to carbonate formation. Zalc et al. [30] attributed the deactivation of Pt/CeO_2 during the WGS reaction to "irreversible" overreduction of CeO_2 by H_2. Our results (Figs. 3a and 3b) disagree with this, because oxidative treatment of the used catalyst results in complete recovery of catalyst activity.

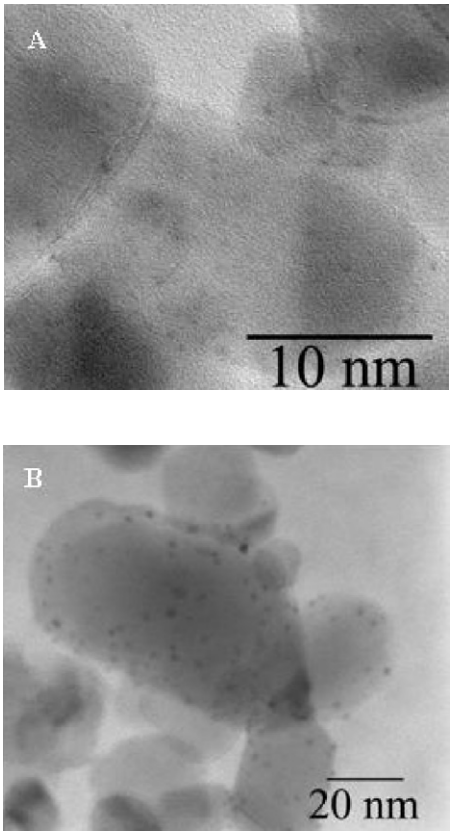

Fig. 4. TEM images of 0.5 Pt/TiO_2, (A) before test and (B) after 20 h test.

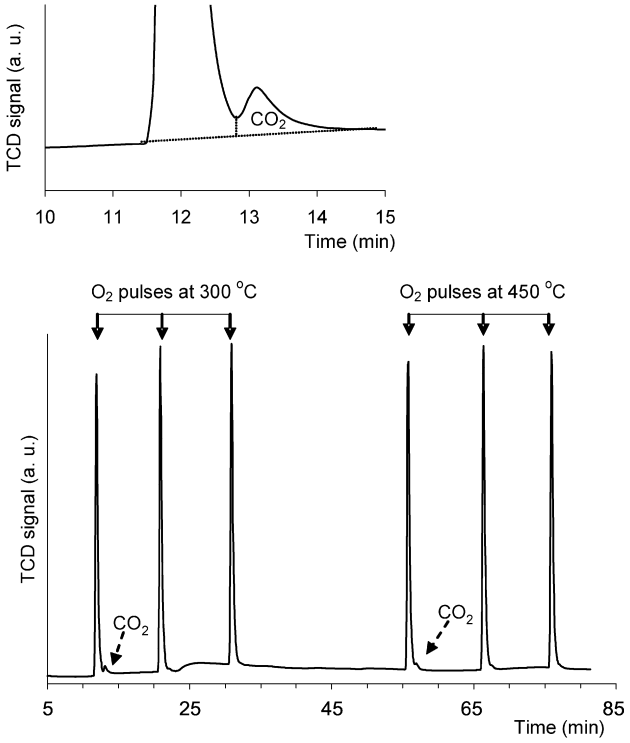

Fig. 5. CO_2 response using TCD observed from the successive pulses of O_2 at 300 and 450 °C on Pt/TiO_2 catalyst after 20 h testing on the stream.

Because formates are reactive intermediates [2], we propose that the deactivation of Pt/CeO_2 catalyst was caused by reactive self-poisoning; CO_2 poisons sites for water sorption/activation via carbonate buildup on ceria. We further propose that this carbonate buildup occurs progressively, blocking ceria sites for the formation of reactive surface formate and thereby causing catalyst deactivation. The poisoning of the active sites is not reversible below 430 °C, the temperature required to decompose ceria carbonate under WGS conditions [29]. This will be a problem for single-stage WGS catalysts operated at lower temperatures, especially because the reactor feed from the hydrocarbon conversion step contains large amounts of CO_2 (2–15% depending on the route to syngas production, i.e., catalytic partial oxidation or steam reforming). The fact that Pt/ZrO_2 is stable (Fig. 3a) agrees with the observations that no stable carbonates are formed during the CO pulses [2] and no Pt sintering occurs (Fig. 3b).

In the case of Pt/TiO_2, carbonate is known to be unstable [31], and thus TiO_2 might have an advantage over ceria as a support in regard to catalyst stability as well as activity. This catalyst deactivated with time (Fig. 3a), however. Its activity could not be restored by heating in oxygen, as was the case for Pt/CeO_2. Pt dispersion decreased during exposure to WGS conditions from 55 to 34% after 20 h of testing (Fig. 3b).

Sintering of Pt was also visible in TEM micrographs for fresh and used Pt/TiO_2 catalysts (Fig. 4). Pt particles had an average size of 1.2 ± 0.2 nm before the 20-h activity test, increasing to 2.7 ± 0.4 nm after the test. Thus, we consider Pt sintering and loss of metal surface area to be the main cause of deactivation.

In the Pt/TiO_2 catalyst, carbon mass balance during kinetic transient experiments [2] indicated that neither coke nor oxygenate species (formates, carbonates) remained on the surface. In addition, to check whether traces of carbon deposition played any significant role in catalyst deactivation, we performed O_2 pulse titration experiments over Pt/TiO_2 after running the catalytic test for 20 h (Fig. 5). To determine the O_2 consumption and product formation, the outlet of the reactor was directly connected to a Porapak column (5 m, 100 °C) and the thermal conductivity detector (TCD). Downstream from the TCD, gases were analyzed by an online mass spectrometer. For the spent Pt/TiO_2 sample, three subsequent O_2 pulses were introduced at 300 °C, after which the temperature was increased to 450 °C and three more O_2 pulses were injected.

The total amount of CO_2 released from the catalyst surface during O_2 pulses at 300 and 450 °C was 2.8 ± 0.1 $\mu mol/g_{cat}$. Recall that the catalyst contained 14 $\mu mol/g_{cat}$ of accessible Pt; thus, CO_2 also could originate from oxidation of "C" species present on Pt. The observed CO_2 corresponded to approximately 20% of the accessible Pt that might be covered with carbon species (i.e., either adsorbed CO or deposited carbon). Obviously, it also was possible that (part of) these deposits resided on the support. Regardless, this carbon species did not cause any catalyst deactivation, because oxidative regeneration did not result in any activity increase (Fig. 3a).

The SMSI effect [i.e., the covering (blockage) of metal Pt by reduced TiO_{2-x} species under reducing conditions] also could be a cause of Pt/TiO_2 deactivation. Typically, this oc-

Table 2
Effect of reduction temperature (T_R) on H_2 chemisorption capacity (H/Pt) of Pt/TiO_2 catalyst (SMSI effect)

T_R (°C)	H/Pt (%)
200	55
250	54
300	54
350	42
400	34
450	15

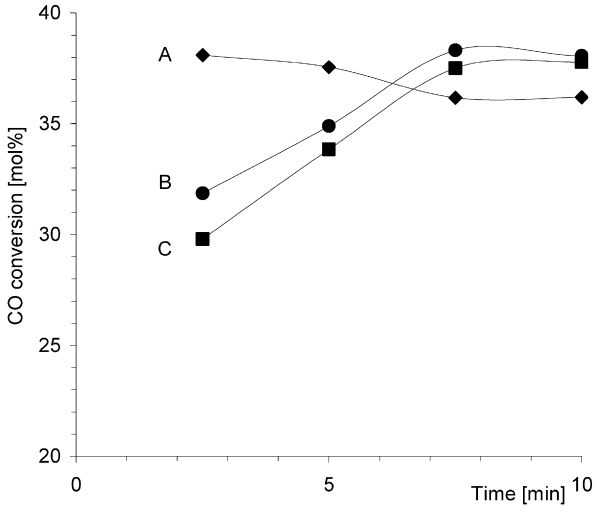

Fig. 6. Effect of reduction temperature (SMSI) on Pt/TiO_2 activity in WGS reaction; using partial pressure of 60 and 150 mbar for CO and H_2O, respectively, $T = 300\,°C$, $P = 2$ bar, and HSGV = 1,050,000 h^{-1}. (A) reduced at 300 °C; (B) reduced at 350 °C; (C) reduced at 400 °C. Lines are just to guide the eye.

curs at above 250 °C for Pt/TiO_2 [32]. Table 2 shows the effect of reduction temperature (T_R) on the hydrogen chemisorption capacity for the Pt/TiO_2 catalyst. Indeed, reduction at temperatures above 300 °C induced SMSI. The chemisorption capacity (H/Pt) dropped from 55 to 15% when the reduction temperature increased from 300 to 450 °C. Fig. 6 shows the catalyst activity (CO conversion) for three different samples of Pt/TiO_2 after reduction at 300, 350, and 400 °C. As shown in this figure, catalyst activity was affected for only few minutes, and rapid reactivation was obvious with time on stream. Thus, the SMSI effect, if present, is almost immediately lost under the WGS reaction conditions. This agrees with the observation by Haller and Resasco [32] that H_2O can reverse the SMSI state. Therefore, we exclude any influence of SMSI on the deactivation observed.

In short, we exclude the possibility that carbon deposits, formation of any stable carbonate, or SMSI contributed to catalyst deactivation. Pt sintering and the corresponding loss of metal surface area was the only cause of the Pt/TiO_2 deactivation. Nonetheless, why Pt did not sinter when supported on CeO_2 or ZrO_2 under similar conditions remains unclear.

Among the mixed-oxide supports, $Ce_{0.5}Ti_{0.5}O_2$ was studied in a more detail. For $Pt/Ti_{0.5}Ce_{0.5}O_2$, the activity and deactivation profile were between those for ceria- and titania-based catalysts. Figs. 3a and 3b show that both Pt sintering and formation of carbonaceous species on the surface caused catalyst deactivation. Oxidative treatment with O_2 at 450 °C for 1 h (Fig. 3a) allowed partial recovery (up to 70%) of initial catalyst activity. Moreover, Pt dispersion for fresh catalyst was 60% and dropped to 47% after 20 h of testing. The role of carbonaceous species on catalyst deactivation is also confirmed by the results of subsequent pulsing of CO and H_2O over $Pt/Ti_{0.5}Ce_{0.5}O_2$ (Fig. 2). During the CO pulses, 687 μmol/g of CO was consumed and 553 μmol/g of CO_2 was formed. As in the case of Pt/CeO_2 [2], no hydrogen was observed. When H_2O was pulsed consecutively, both H_2 and CO_2 (30 $\mu mol/g_{cat}$) were observed. Carbon mass balance indicated that 15% of the CO introduced (104 $\mu mol/g_{cat}$) was retained on the catalyst surface as carbonaceous species, causing a loss of active sites and inducing deactivation.

These observations confirm that, similar to the findings for catalyst activity discussed above, the stability of mixed-oxide based catalysts were again between that of the single-oxide based catalysts. The mixed oxide was at least partly truly mixed, as discussed above as well. Nevertheless, it is obvious that no synergy whatsoever was obtained for both activity and stability.

3.3. Development of a stable and efficient catalyst

The Pt/TiO_2 catalyst can be considered a promising catalyst for industrial applications in single-stage WGS, provided that Pt dispersion on titania can be maintained under WGS conditions. For Pt/Al_2O_3-reforming catalysts, deactivation has been attributed to Pt sintering and coke formation. It has been recognized that adding a second metal [i.e., rhenium (Re) or tin (Sn)] can improve the lifetime of Pt/Al_2O_3 through preventing sintering by occupying Pt grain boundaries and suppressing coke formation by promoting hydrogenation of coke precursors [33–39]. Rezgui et al. [34] and Reitmaier et al. [35] reported that the Pt–O–Al bond is strengthened by the addition of Re, which helps anchor the Pt and maintain its dispersion. Further conversion of carbonaceous species on the support surface to the more inert graphitic carbon is suppressed. Coq and Figueras [38] and Dautzenberg et al. [39] proposed that adding Sn on Pt/Al_2O_3 changes the intrinsic catalytic properties of Pt, weakening the Pt–C bond during reforming reactions and leading to changes in selectivity and reduced coke formation on platinum. Recent studies [40,41] reported that the activity of Pt/TiO_2 catalyst for the WGS reaction can be enhanced by the addition of Re; however the reason for the improved catalyst activity remains unclear. Moreover, catalyst stability was not discussed at all.

Fig. 7 shows the WGS activity for 0.5% Pt/TiO_2, 0.5% Pt–0.48% Re/TiO_2, 0.5% Re/TiO_2, and 0.5% Pt–0.3% Sn/TiO_2 catalysts as function of time on stream at 300 °C. The figure clearly shows that adding Re to Pt/TiO_2 improved catalyst stability. The catalysts showed almost no deactivation during 20 h time on stream. The Pt–Sn/TiO_2 catalyst was also stable, but because it demonstrated very low activity, it is of no further interest. To check the influence of Re on the Pt/TiO_2 catalyst, Pt dispersion was measured for both the Pt/TiO_2 and Pt–Re/TiO_2 catalysts before and after the 20-h activity test (Fig. 8). Both

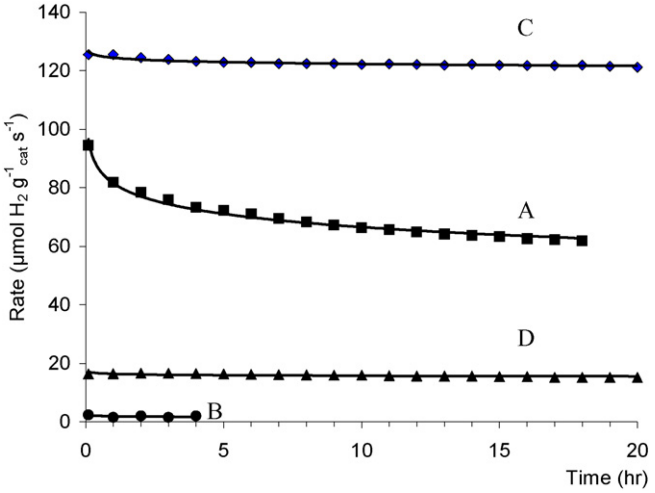

Fig. 7. WGS rates at 300 °C as a function of time on stream for (A) 0.5% Pt/TiO_2; (B) 0.5% Re/TiO_2 (C) 0.5% Pt–0.48% Re/TiO_2; (D) 0.5% Pt–0.3% Sn/TiO_2 catalysts. Conditions: partial pressure of 60 and 150 mbar for CO and H_2O, respectively, $P = 2$ bar, and HSGV = 410,000 h^{-1}.

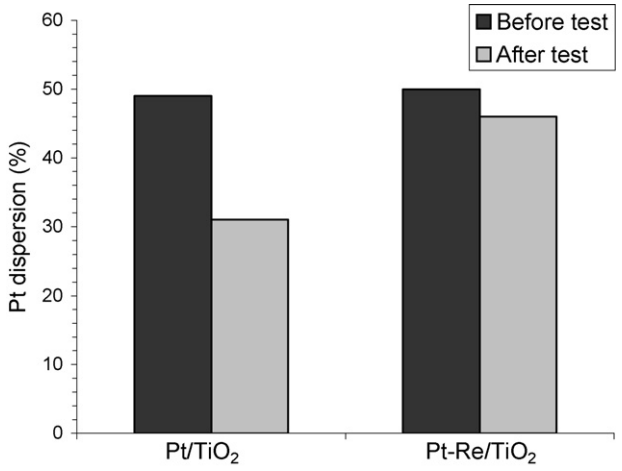

Fig. 8. Pt dispersion of 0.5% Pt/TiO_2 and 0.5% Pt–0.48% Re/TiO_2 using CO chemisorption; before test and after 20 h test on the stream.

catalysts demonstrated almost identical Pt dispersion before testing: 49% for Pt/TiO_2 and 50% for Pt–Re/TiO_2. After the activity tests, Pt/TiO_2 lost 36% (relative loss) of the initial Pt dispersion; Pt–Re/TiO_2 was affected much less significantly (8% loss). TEM measurements on fresh and deactivated Pt–Re/TiO_2 catalysts confirmed this finding (Fig. 9). Pt particles on Pt–Re/TiO_2, before and after the 20-h test had an average size of 2.1 ± 0.3 nm. These findings demonstrate that the addition of Re indeed improved the stability of Pt particles by preventing sintering.

It is remarkable that Re not only stabilized the Pt/TiO_2 catalyst, but also enhanced activity, that is, the rate of H_2 production. By itself, Re/TiO_2 demonstrated no activity in the WGS reaction (Fig. 7). In our case, the activity increase for Pt–Re/TiO_2 was not due to improved Pt dispersion in the presence of Re, as claimed by Iida and Igarashi [40]. The two catalysts tested, Pt/TiO_2 and Pt–Re/TiO_2, had very similar Pt dispersions but differing activities (95 and 125 μmol $H_2/(g_{cat}\ s)$, respectively).

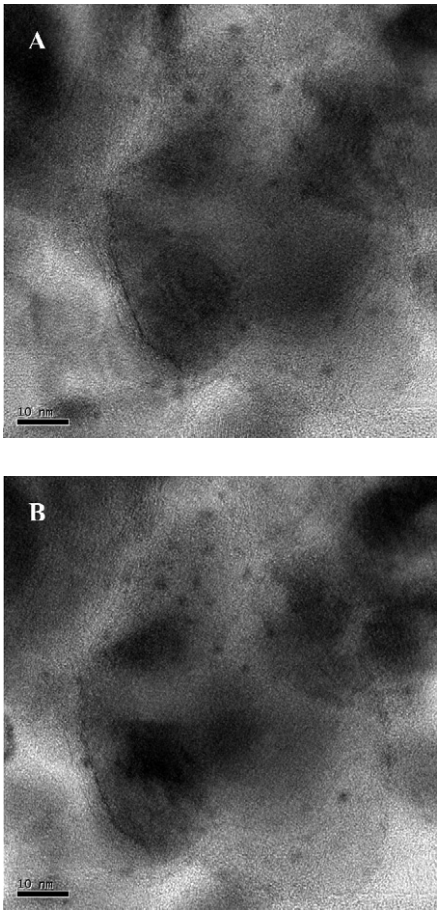

Fig. 9. TEM images of 0.5% Pt–0.48% Re/TiO_2: (A) before test and (B) after 20 h test.

To elucidate the role of Re in the WGS reaction sequence, it is essential to determine the form in which it is present in the Pt–Re/TiO_2 catalyst under in situ WGS conditions. Based on XPS and XAS techniques, Onuferko et al. [42] found that the Re in Pt–Re/Al_2O_3 existed in an oxidized state (IV) even after in situ reduction at 485 °C. An ESR study by Nacheff et al. [43] also confirmed the existence of Re (IV) along with Re (0) in Pt–Re/Al_2O_3 reduced at 500 °C. Huang et al. [44] showed, by TEM/EDX analysis, that most of the Re in Pt–Re/Al_2O_3 reduced at 400 °C was present as ReO_2.

Our own XPS measurements of 0.5% Re/TiO_2, 0.5% Pt/TiO_2, and 0.5% Pt–0.48% Re/TiO_2 after ex situ reduction with H_2 at 300 °C also suggest that at least part of Re was present as ReO_x (Fig. 10). Fig. 11 shows the TPR profile of Pt–Re/TiO_2 catalyst. The reduction profile is complex, with four different reduction stages. In accordance with data reported previously [26,45,46], the first peak corresponds to reduction of Pt, and the three subsequent peaks correspond to reduction of ReO_x. Two observations are important for our current discussion: (i) Complete reduction of ReO_x to Re^0 occurs only above 500 °C, and (ii) part of the ReO_x can be reduced under WGS conditions (300 °C/H_2). We speculate that ReO_x provides an additional reaction pathway for H_2O sorption/activation and thereby improves the catalyst activity. This is a subject of ongoing detailed investigation.

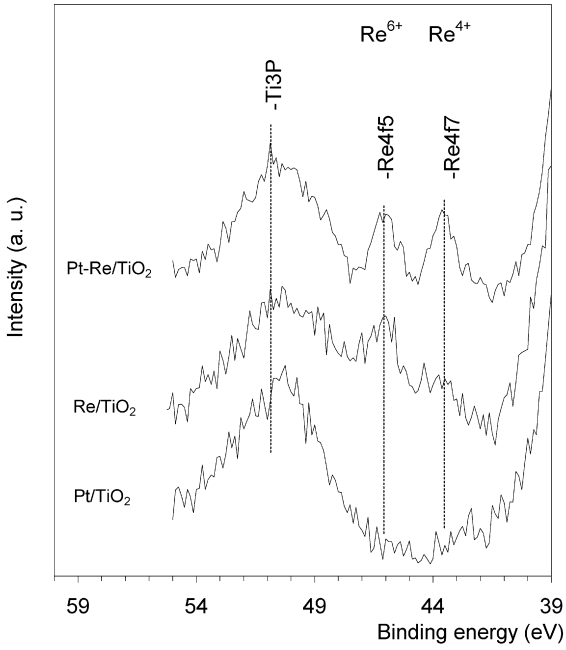

Fig. 10. XPS spectra for Re 4f in 0.5% Pt/TiO_2, 0.5% Re/TiO_2 and 0.5% Pt–0.48% Re/TiO_2 catalysts after reduction at 300 °C.

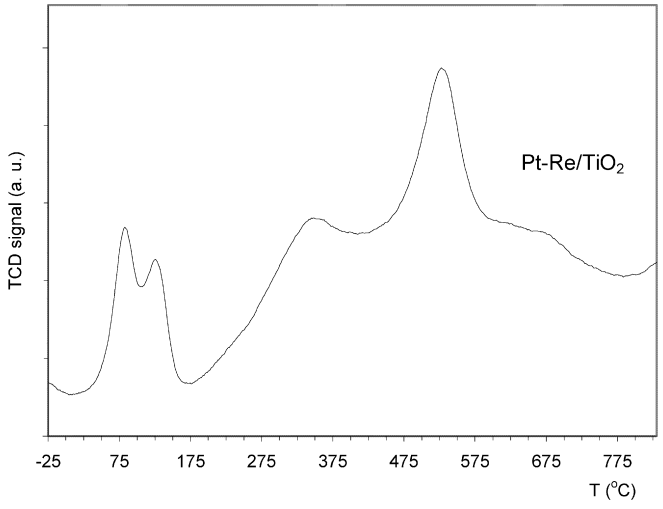

Fig. 11. H_2-TPR profile of Pt–Re/TiO_2. Heating rate was 10 °C/min; gas contains 15% H_2 in Ar. The gas flow was 20 ml/min.

4. Conclusion

Our findings indicate that the nature of the oxide support has a significant influence on the activity and stability of the catalysts in the WGS reaction. The Pt/TiO_2 catalyst showed the best activity for the WGS reaction among the catalysts studied, even better than Pt/CeO_2, which is often cited as a promising catalyst for fuel cell applications. Using mixed oxides as catalyst supports did not improve the activity despite the enhanced red–ox properties of the mixed-oxide supports compared with the single-oxide supports.

The Pt/CeO_2 catalyst suffered from deactivation caused by self poisoning, that is, formation of stable carbonate on the ceria surface. The surface carbonates blocked the WGS reaction sequence by preventing the creation of seemingly crucial formate intermediates. Carbonates caused no deactivation on the Pt/TiO_2 catalyst, because carbonates were not stable on titania under WGS temperatures. Pt/TiO_2 deactivation was caused by Pt sintering exclusively. Accordingly, the stability of Pt/TiO_2 can be improved by adding Re, which prevents Pt sintering. In addition, the presence of Re increased the catalytic activity of Pt/TiO_2. We propose that part of the Re was present under reaction conditions in oxidized form (ReO_x).

Acknowledgments

The authors thank Ing. L. Vrielink for the XRF and BET analyses, Ing. M. Smithers for the TEM measurements, and Ing. B. Geerdink and K. Altena-Schildkamp for technical assistance. Financial support was provided by STW (project 790.36.030).

References

[1] C.H. Bartolomew, R.J. Farrauto, in: C.H. Bartolomew, R.J. Farrauto (Eds.), Fundamentals of Industrial Catalytic Processes, Wiley, Hoboken, NJ, 2006, p. 909.
[2] K.G. Azzam, I.V. Babich, K. Seshan, L. Lefferts, J. Catal. 251 (2007) 153 (part 1 of this paper).
[3] M.A. Henderson, Surf. Sci. Rep. 46 (2002) 1.
[4] T. Bunluesin, R.J. Gorte, G.W. Graham, Appl. Catal. B 15 (1998) 107.
[5] P. Panagiotopoulou, D.I. Kondarides, Catal. Today 112 (2006) 49.
[6] G. Jacobs, U.M. Graham, E. Chenu, P.M. Patterson, A. Dozier, B.H. Davis, J. Catal. 229 (2005) 499.
[7] G. Jacobs, L. Williams, U. Graham, G.A. Thomas, D.E. Sparks, B.H. Davis, Appl. Catal. A Gen. 252 (2003) 107.
[8] T. Shido, Y. Iwasawa, J. Catal. 141 (1993) 71.
[9] D. Tibiletti, A. Goguet, D. Reid, F. Meunier, R. Burch, Catal. Today 113 (2006) 94.
[10] G. Jacobs, A. Crawford, L. Williams, P.M. Patterson, B.H. Davis, Appl. Catal. A Gen. 267 (2004) 27.
[11] P. Panagiotopoulou, A. Christodoulakis, D.I. Kondarides, S. Boghosian, J. Catal. 240 (2006) 114.
[12] E. Xue, M. O'Keeffe, J.R.H. Ross, Surf. Sci. Catal. 130 (2000) 3813.
[13] G. Jacobs, S. Ricote, B.H. Davis, Appl. Catal. A 302 (2006) 14.
[14] H. Iida, K. Kondo, A. Igarashi, Catal. Commun. 7 (2006) 240.
[15] O. Goerke, P. Pfeifer, K. Schubert, Appl. Catal. A 263 (2004) 11.
[16] D. Martin, D. Duprez, J. Phys. Chem. 100 (1996) 9429.
[17] M. Calatayud, A. Markovits, M. Menetrey, B. Mguig, C. Minot, Catal. Today 85 (2003) 125.
[18] L. Mattos, E.R. Oliveira, P.D. Resende, F.B. Noronha, F.B. Passos, Catal. Today 77 (2002) 245.
[19] K. Takanabe, K. Aika, K. Inazu, T. Baba, K. Seshan, L. Lefferts, J. Catal. 227 (2004) 101.
[20] S. Pengpanich, V. Meeyoo, T. Riraksomboon, K. Bunyakiat, Appl. Catal. A Gen. 234 (2002) 221.
[21] A. Wootsch, C. Descorme, D. Duprez, J. Catal. 225 (2004) 259.
[22] W. Ruettinger, X. Liu, R. Robert, J. Farrauto, Appl. Catal. B Environ. 65 (2006) 135.
[23] G. Dong, J. Wang, Y. Cao, S. Chen, Catal. Lett. 58 (1999) 37.
[24] D. Teschner, A. Wootsch, T. Roder, K. Matusek, Z. Paal, Solid State Ionics 141–142 (2001) 709.
[25] C.L. Pieck, C.R. Vera, J.M. Perera, G.N. Gimenez, L.R. Serra, L.S. Carvalho, M.C. Rangel, Catal. Today 107–108 (2005) 637.
[26] L.S. Carvalho, C.L. Pieck, M.C. Rangel, N.S. Figoli, J.M. Grau, P. Reyes, J.M. Parera, Appl. Catal. A Gen. 269 (2004) 91.
[27] R.J. Gorte, S. Zhao, Catal. Today 104 (2005) 18.
[28] D.C. Grenoble, M.M. Estadt, D.F. Ollis, J. Catal. 67 (1981) 90.
[29] X. Liu, W. Ruettinger, X. Xu, R. Farrauto, Appl. Catal. B Environ. 56 (2005) 69.

[30] J.M. Zalc, V. Sokolovskii, D.G. Loffler, J. Catal. 206 (2002) 169.
[31] J.A. Wang, A. Cuan, J. Salamones, N. Nava, S. Castillo, M. Moran-Pineda, F. Rojas, Appl. Surf. Sci. 230 (2004) 94.
[32] G.L. Haller, D.E. Resasco, Adv. Catal. 36 (1989) 173.
[33] C. Audo, J.F. Lambert, M. Che, B. Didillon, Catal. Today 65 (2001) 157.
[34] S. Rezgui, R. Jentoft, B.C. Gates, J. Catal. 136 (1996) 496.
[35] S.F. Reitmaier, A. Subramaniam, P.A. Sermon, Catal. Today 19 (1993) 345.
[36] H. Dexpert, P. Lagarade, J. Mol. Catal. 25 (1984) 347.
[37] C.L. Pieck, P. Marecot, C.A. Querini, J.M. Peraera, Appl. Catal. A Gen. 133 (1995) 281.
[38] B. Coq, F. Figueras, J. Catal. 85 (1984) 197.
[39] F.M. Dautzenberg, J.N. Helloen, W.M.H. Sachtler, J. Catal. 63 (1980) 119.
[40] H. Iida, A. Igarashi, Appl. Catal. A Gen. 303 (2006) 192.
[41] Y. Sato, K. Terada, S. Hasegawa, T. Miyao, S. Naito, Catal. Commun. 7 (2006) 91.
[42] J.H. Onuferko, Appl. Surf. Sci. 19 (1984) 227.
[43] M.S. Nacheff, L.S. Kraus, M. Ichikawa, B.M. Hoffman, J.B. Butt, W.M.H. Sachtler, J. Catal. 106 (1987) 263.
[44] Z. Huang, J.R. Fryer, C. Park, D. Stirling, G. Webb, J. Catal. 148 (1994) 478.
[45] P. Reyes, G. Pecchi, M. Morales, J.L.G. Fierro, Appl. Catal. A Gen. 163 (1997) 145.
[46] C.L. Pieck, C.R. Vera, J.M. Parera, G.N. Gimenez, L.R. Serra, L.S. Carvalho, M.C. Rangel, Catal. Today 107–108 (2005) 637.